



71st Conference of the Italian Thermal Machines Engineering Association, ATI2016, 14-16
September 2016, Turin, Italy

CFD modeling of the supersonic condensation inside a steam ejector

Francesco Giacomelli^a, Giulio Biferi^a, Federico Mazzelli^a, Adriano Milazzo^{a*}

^aUniversity of Florence, Department of Industrial Engineering of Florence (DIEF),
via di S. Marta 3, 50139, Firenze, Italy.

Abstract

Supersonic steam ejectors are commonly used in many applications, for example suction of non-condensable gases in steam power plants or heat-powered chillers. In the specific case of ejector chillers, CFD studies of the ejector are necessary for optimization of this device because ejector performances have a direct impact on the COP of the chiller. The complex ejector flow and the high Mach numbers make characterization of the phase change inside this component difficult. Metastability effects also have to be accounted for and some CFD commercial software provide built-in wet-steam models for this purpose. A simpler approach for numerical modeling of multiphase ejector is the Homogeneous Equilibrium Model (HEM) in which the phase change occurs in equilibrium conditions, i.e. metastability is neglected. These second kinds of models are still important tools for preliminary analysis of condensing ejectors. In the present paper a comparison between commercial software wet-steam models and an in-house developed model based on HEM is presented.

© 2016 The Authors. Published by Elsevier Ltd. This is an open access article under the CC BY-NC-ND license (<http://creativecommons.org/licenses/by-nc-nd/4.0/>).

Peer-review under responsibility of the Scientific Committee of ATI 2016.

Keywords: supersonic ejectors, CFD, numerical modeling, non-equilibrium condensation, wet-steam;

1. Introduction

Ejector refrigerators are able to utilize waste heat to produce cooling. Steam driven variants are used by the food processing industry to freeze dry products and for many years they were used on-board ships to provide both process cooling and air conditioning. The choice of water as a refrigerant has obvious advantages with regard to environmental

* Corresponding author. Tel.: +39-055-2758738.
E-mail address: adriano.milazzo@unifi.it.

Nomenclature	
β	liquid mass fraction
η	total number of droplets per unit volume
ρ_{mix}	mixture density
R	gas constant
T_{SAT}	saturation temperature
P_{SAT}	saturation pressure

regulations and fluid costs. Moreover, a recent study has shown that steam ejector plants may have better performances than systems using synthetic refrigerants [1].

The scheme of a standard Steam Ejector Cycle is shown in Fig. 1 along with its corresponding T-s diagram. Basically, the whole system can be thought as composed of two parts, the power and refrigeration cycles. The two cycles share the condenser and the power exchange between them occurs by means of a supersonic ejector. System performance can be quantified by means of the Coefficient Of Performance (COP) which is defined as the cooling load divided by the total heat and mechanical power inputs:

$$COP = \frac{\dot{Q}_{\text{eva}}}{\dot{Q}_{\text{gen}} + \dot{W}_{\text{pump}}} \approx \frac{\dot{m}_s \Delta h_{\text{eva}}}{\dot{m}_p \Delta h_{\text{eva}}} \tag{1}$$

The ratio between the suction mass flow rate, \dot{m}_s , to the motive mass flow rates, \dot{m}_p , defines the Entrainment Ratio (ER), which is a fundamental parameter for the performance of the ejector as it is proportional to the system COP.

For more details on the system operations and on the ejector dynamics the reader can refer to [2].

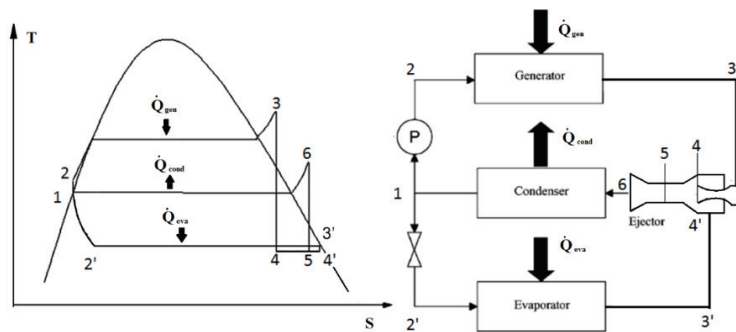


Figure 1: T-s diagram and basic scheme of a standard steam ejector cycle

As can be seen in Fig. 1, normal operation of a steam ejector involves expansions, mixing and compressions that occur well within the saturation dome. In the ideal case of a reversible transformation, the condensation process follows a path of equilibrium states, and no losses occur. Inside supersonic ejectors. However, the very limited residence time and high cooling rates lead to a substantial departure from the equilibrium process. As the primary

flow rapidly expands inside the motive nozzle, thermodynamic equilibrium is not maintained and, at a certain degree of expansion, the vapor state collapses and condensation takes place abruptly as a shock-like disturbance [3]. This is generally called the “condensation shock”. This sudden change of state of aggregation leads to an instantaneous and localized heat release that increase the pressure and temperature and reduce the Mach number along the ejector [3].

Downstream the condensation shock, the flow contains a considerable number of tiny liquid droplets (of the order of $10^{19}=\text{dm}^3$, [4]) that affect the turbulence levels and the subsequent shear layer development in the mixing chamber [5]. Therefore, in addition to a reduction of the nozzle efficiency, condensation can also have consequences on the entrainment of the suction flow. Consequently, a reliable design technique for condensing ejectors should be able to account for all these effects. Unfortunately, to date no such scheme has been devised. As a consequence, the design is ultimately conducted by making use of empirical prescriptions or correlations of experimental data (e.g. [6]).

This work represents an attempt to overcome all or some of these limitations. To this aim, a CFD code that includes a non-equilibrium condensation model is tested in order to assess and refine the performances of a “first-attempt” ejector design obtained by a 1D model procedure.

2. Homogenous Equilibrium Model

The Homogeneous Equilibrium Model (HEM) is an Eulerian model to study equilibrium phase change. Due to its simplicity it can be used as a valid approach to obtain results in a preliminary stage of the ejector designing process. Its main limitations can be summarized as follows:

- Phases in mechanical equilibrium, i.e., they have the same velocity;
- Phases in thermodynamic equilibrium, i.e., they have the same temperature;
- No possibility to account for metastability affects.

In particular, this last approximation may lead to significant errors due to the high speed that occurs within supersonic ejectors. This point is studied in details in the Results chapter.

The implementation of the HEM in ANSYS Fluent [7] can be done by simulating a fluid with mean properties between liquid and vapor, which is function of pressure and static enthalpy [J/kg] (for more details see [8]). The default Energy equation in ANSYS Fluent is replaced with a user defined scalar transport equation where the only unknown variable is the specific enthalpy:

$$\nabla \cdot (\rho \tilde{u} \tilde{h}) = \nabla \cdot (\Gamma_{h,eff} \nabla \tilde{h}) + \dot{S}_{h1} + \dot{S}_{h2} + \dot{S}_{h3} \quad (2)$$

$$\dot{S}_{h1} = \tilde{u} \cdot \nabla \bar{p}$$

$$\dot{S}_{h2} = (\mu + \mu_T) \left\{ 2 \left[\left(\frac{\partial \tilde{u}}{\partial x} \right)^2 + \left(\frac{\partial \tilde{v}}{\partial y} \right)^2 + \left(\frac{\partial \tilde{w}}{\partial z} \right)^2 \right] + \left(\frac{\partial \tilde{u}}{\partial y} + \frac{\partial \tilde{v}}{\partial x} \right)^2 + \left(\frac{\partial \tilde{u}}{\partial z} + \frac{\partial \tilde{w}}{\partial x} \right)^2 + \left(\frac{\partial \tilde{v}}{\partial z} + \frac{\partial \tilde{w}}{\partial y} \right)^2 - \frac{2}{3} (\nabla \cdot \tilde{u})^2 \right\} - \frac{2}{3} \rho K \nabla \cdot \tilde{u}$$

$$\dot{S}_{h3} = -\rho \tilde{u} \cdot \nabla K$$

Where (\sim) and $(-)$ denote Favre- and Reynolds-averaged quantities, \mathbf{u} is the velocity vector and u, v, w are its components. ρ is the local density, μ and μ_T are the molecular and turbulent viscosity respectively. $\Gamma_{h,eff}$ is the effective diffusion coefficient, which represents the sum of the molecular and turbulent thermal diffusion coefficients. As for the fluid properties, these have been implemented as follows:

- density defined via User-Defined Function (UDF) as a function of pressure and specific enthalpy;
- speed of sound defined via User-Defined Function (UDF) as a function of pressure and specific enthalpy;

- Average vapor phase value for the molecular viscosity and molecular diffusion coefficient.

The last assumption is practically equivalent to consider “dry walls” due to the heat recovery in the boundary layer (due to the high turbulence levels, the molecular diffusion and viscosity affects only the dynamics of the viscous sub-layer).

The introduction of the sound speed formulation is required by ANSYS Fluent to solve the pressure-correction equation. Unfortunately, formulation of the two-phase speed of sound are not available within REFPROP libraries. Therefore, in the two-phase region, the sound speed has been calculated from an equation which is widely used in mixture models (for example [9]):

$$c = \sqrt{\frac{1}{\rho \left(\frac{\alpha_v}{\rho_v c_v^2} + \frac{1 - \alpha_v}{\rho_l c_l^2} \right)}} \tag{3}$$

Where α_v is the vapor volume fraction, ρ_v and ρ_l are respectively vapor and liquid density for a given pressure, c_v and c_l are respectively vapor and liquid sound speed for a given pressure.

From a numerical point of view, both density and sound speed are calculated by means of lookup-tables constructed by developing an in-house Matlab code that automatically generates the fluid property matrices by acquiring data from REFPROP libraries. The CFD solver then operates a bi-linear interpolation (with pressure and specific enthalpy as independent variables) to obtain the correct value of density and sound speed in each cell of the computational domain.

3. Wet Steam model

Wet steam models are Eulerian homogeneous models available in many commercial CFD software. In the present work, the Wet Steam model built in ANSYS Fluent v16.2 was used for all simulations. The model considers the condensed phase as monodispersed in the vapor phase. The transport equations are written for the whole mixture whose properties result from mass weighted averages of each phase. In order to account for metastable phase change two additional transport equations are coupled to the standard set of compressible Navier-Stokes equations:

$$\frac{\partial \rho_{mix} \beta}{\partial t} + \nabla \cdot (\rho_{mix} \vec{u} \beta) = \Gamma \tag{5}$$

$$\frac{\partial \rho_{mix} \eta}{\partial t} + \nabla \cdot (\rho_{mix} \vec{u} \eta) = \rho_{mix} J \tag{6}$$

Where Γ and J are the source terms representing the mechanism of droplets nucleation and growth, respectively. These formulations are derived by means of kinetic and thermodynamic concepts (for more details see [10], [11], [7]).

The equation of state for the steam is calculated based on a Virial equation of state truncated at the third term of the expansion and calibrated following the work of Young [12]:

$$p = \rho_{mix} RT \cdot (1 + B \rho_{mix} + C \rho_{mix}^2) \tag{7}$$

Where B and C are the second and third Virial coefficients.

By making use of the Virial equation it is possible to describe metastable states of the steam by simply extrapolating the validity range of the equation for regions below the saturation curve. In the range of conditions usually attained in low pressure steam turbines, the equation remains well behaved and no anomalies should be expected [13]. All

the other properties (density for vapor and liquid, specific heats etc.) are calculated with correlations which are functions of the local temperature.

A notable limitation of the wet steam model is that it is not capable to evaluate the ice formation. This implies that liquid temperature should remain always greater than triple point temperature (273.15 K), as long as no metastability effects are assumed for the solidification process. A further restrictive assumption of the model is the limit to the maximum liquid mass fraction, which should be limited to values no greater than 0.1-0.2 for reasons of numerical stability.

4. Numerical setup

CFD analyses are performed with ANSYS Fluent v.16.2. The computational domain is two-dimensional and axis-symmetric, the mesh is composed of approximately 45000 quadrilateral elements and is wall resolved. The solver adopted for the Wet-Steam calculations is a density based solver while in case of the HEM approach the solver is pressure-based with a pressure velocity coupling. Calculations are second order accurate and a $k-\omega$ SST turbulence model is selected in all cases because it was seen to give good results in previous ejector studies [14]. The boundary conditions at the inlets are summarized in Table 1. The inlets pressures are the saturation pressures corresponding to T_{SAT} and they are maintained as constants for various outlet pressures.

	T_{SAT} [°C]	T_{SH} [°C]
Primary Inlet	80	1
Secondary Inlet	7	0

Table 1: Boundary conditions at the inlets of the ejector

5. Results

Fig. 1 shows a comparison of the entrainment ratio data between the Wet Steam (WS) and the Homogeneous Equilibrium Model (HEM). The HEM predicts a lower value of this quantity. The mismatch is connected mainly to differences in the prediction of the velocity profiles at the Nozzle Exit Plane. In turn, these are most likely due to the different equation of state and fluid properties (and in particular, the heat capacity ratio) which causes different expansion levels and results in different mass flow rates in the nozzle throat.

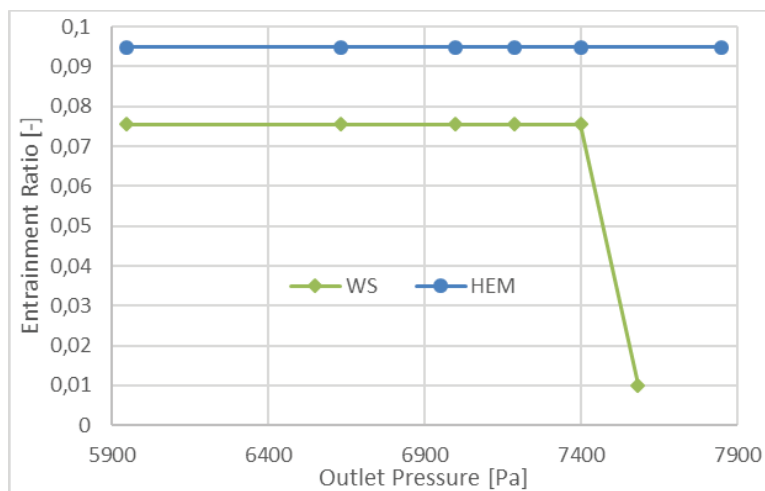


Fig. 1: Entrainment Ratio of the ejector for different outlet pressures

Fig. 2 shows the variation of density along the nozzle axis. The throat region is highlighted in red in order to show that the density differences are almost negligible at this point, thus confirming that the mass flow rate discrepancies are mostly affected by velocity trends. Right downstream the throat region a clear mismatch in the density profiles is visible. The main reason for this is to be found in the WS model capacity to account for metastability effects, which results in the aforementioned “condensation shock”. As can be seen, this amounts to an abrupt variation of density during the phase change process, as opposed to the gradual variation of the HEM.

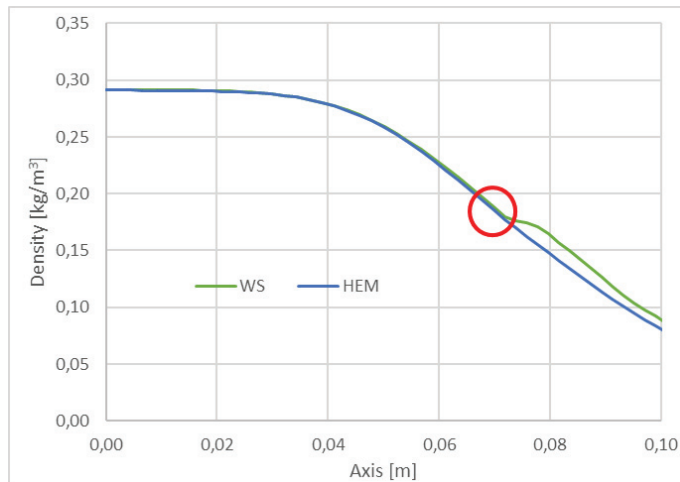


Fig. 2: Comparison of density trends along the axis (the red circle highlights the nozzle throat region)

Fig. 3 shows the quality contour inside the ejector. Clearly, the HEM overestimates the variations of quality with respect to the WS model. Due to the assumption of thermodynamic equilibrium, the HEM model gives rise to instantaneous quality variation that follows the compressions and expansion patterns in the mixing chamber. On the other hand, the Wet Steam model accounts for the time dependency of the condensation process (i.e., relaxation time), hence, the shocks have a lower impact on the quality (and, of course, on the other flow variables). This difference in the model behavior results in significant discrepancies in the pressure profile along the axis, as shown in Fig. 4. In other words, the relaxation time included within the WS model acts as a damper in the shock/expansion processes that occur all along the ejector length.

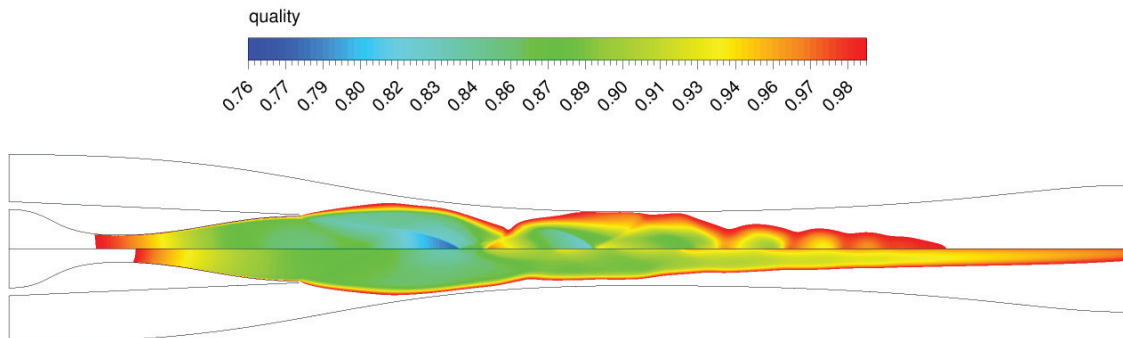


Fig. 3 Contours of quality; HEM up, WS down

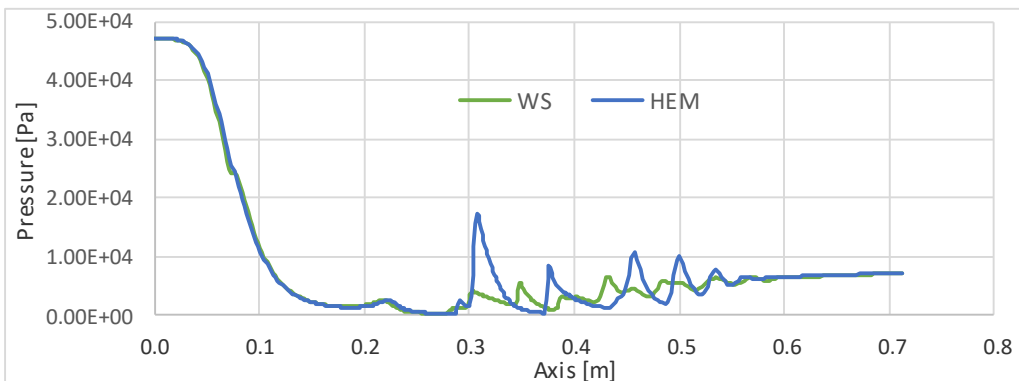


Fig. 4: Comparison of pressure trends along the axis

Fig. 5 shows a comparison of the temperature results along the axis. In the case of Wet Steam model the temperature goes well below the HEM results. This is again due to the absence of a relaxation time of HEM: due to the higher variation of the quality, the condensing mass is generally higher in HEM, thus resulting in higher latent heat transfer and lower temperatures. Most interestingly, looking at the WS profile of both vapor and liquid phase one can see that the temperatures go well below the Triple Point temperature in some regions downstream the nozzle exit (273.15K), meaning that there are some possibilities of ice formation inside the ejector.

It is interesting to note that the temperature of the liquid phase for the WS are very close to that of the HEM model. This is probably due to the fact that the Fluent WS model assumes the liquid temperature to be the equilibrium saturation temperature at the vapor pressures. Therefore, whenever the pressure differences between the two models are small, the two temperatures are close to each other (this is true as long as the system is two phase).

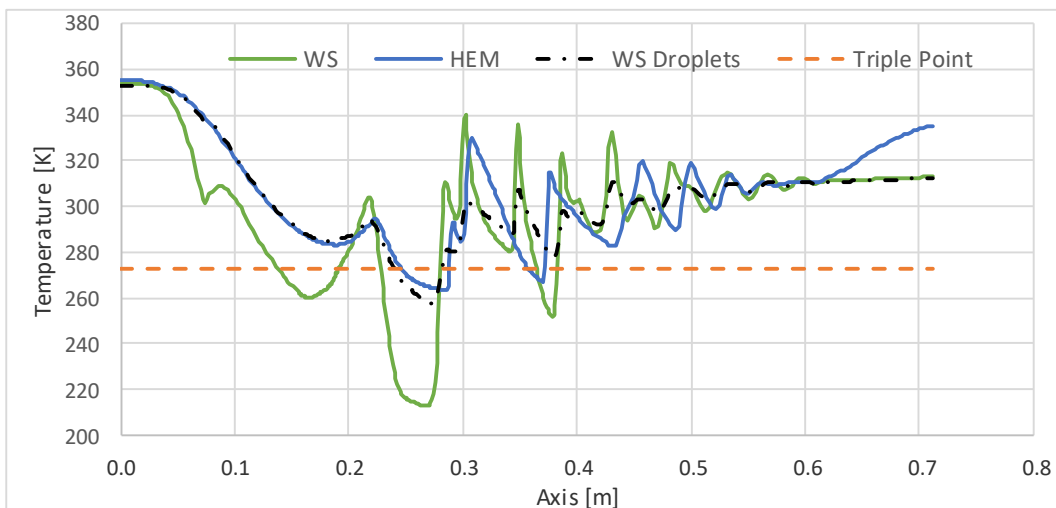


Fig. 5: Comparison of temperature trends along the axis

6. Conclusions

Steam ejectors are widely used in many industrial applications and CFD studies are necessary for the optimization of these devices. In the present paper a comparison of two different approaches to account for the condensation inside a supersonic steam ejector is proposed. The first approach involves the Wet Steam Model while the second is a Homogeneous Equilibrium Model, which was implemented in the commercial code ANSYS Fluent by means of User-Defined functions.

The results have shown that HEM overestimates the variations of the main quantities during the shocks/expansion process occurring in the ejector. On the other hand, the WS model considers the time-dependency of the condensation phenomena, thus resulting in the presence of a condensation shock downstream the primary nozzle throat. Moreover, the relaxation times connected with the non-equilibrium model results in a smoother variation of pressure and quality along the axis with respect to HEM results. Finally, the lower condensation predicted by the WS model results in lower temperature during the expansion compared to the results of the HEM. The temperature of both phases goes below the Triple Point temperature, meaning that there is the possibility of ice formation in the ejector.

Although the HEM is a simplified approach which is not able to account for metastability effects, nevertheless it can still reproduce most of the main features of the flow dynamics. Moreover, it is more stable (from a numerical point of view) and easily adaptable to various fluids, hence it could be regarded as a preliminary design tool.

References

- [1] M. Milazzo and A. Rocchetti, "Modelling of ejector chillers with steam and other working fluids," *International Journal of Refrigeration*, vol. 57, pp. 277-287, 2015.
- [2] F. Mazzelli and A. Milazzo, "Performance analysis of a supersonic ejector cycle working with R245fa," *International Journal of Refrigeration*, vol. 49, pp. 79-92, 2015.
- [3] P. Wegener and L. Mack, *Condensation in supersonic and hypersonic wind tunnels*, New York: Academic Press Inc., 1958.
- [4] P. G. Hill, "Condensation of water vapour during supersonic expansion in nozzles," *Journal of Fluid Mechanics*, vol. 25, pp. 593-620, 1966.
- [5] C. Crowe, J. Schwarzkopf, M. Sommerfeld and Y. Tsuji, *Multiphase flow with droplets and particles*, Second edition, CRC Press, 2012.
- [6] ESDU item number 86030, *Ejectors and jet pumps. Design for steam driven flow*, 1986.
- [7] ANSYS Inc., *ANSYS Fluent Theory Guide*, Canonsburg, PA: release 16.2, 2009.
- [8] F. Giacomelli, F. Mazzelli and A. Milazzo, "Evaporation in supersonic CO₂ ejectors: analysis of theoretical and numerical models," in *International Conference on Multiphase Flow*, Firenze, Italy, 2016.
- [9] S. Yakubov, T. Maquil and T. Rung, "Experience using pressure-based CFD methods for Euler-Euler simulations of cavitating flows," *Computers & Fluids*, vol. 111, pp. 91-104, 2015.
- [10] L. Zori and F. Kececy, "Wet Steam Flow Modeling in a General CFD Flow Solver," in *35th AIAA Fluid Dynamics Conference and Exhibit*, Toronto, Canada, 2005.
- [11] Y. Yang and S. Shen, "Numerical simulation on non-equilibrium spontaneous condensation in supersonic steam flow," *International Communications in Heat and Mass Transfer*, vol. 36, pp. 902-907, 2009.
- [12] J. B. Young, "The spontaneous condensation of steam in supersonic nozzles," *Physico Chemical hydrodynamics*, vol. 3, pp. 57-82, 1982.
- [13] J. B. Young, "An equation of state for steam for turbomachinery and other flow calculations," *Trans. ASME, Journal of Engineering Gas Turbines and Power*, vol. 110, pp. 1-7, 1988.
- [14] F. Mazzelli, A. B. Little, S. Garimella e Y. Bartosiewicz, «Computational and Experimental Analysis of Supersonic Air Ejector: Turbulence Modeling and Assessment of 3D Effects,» *International Journal of Heat and Fluid Flow*, vol. 56, pp. 305-316, 2015.